THE JOURNAL OF BIOLOGICAL CHEMISTRY VOL. 290, NO. 14, pp. 9122–9134, April 3, 2015


# Phosphorylation of Targeting Protein for *Xenopus* Kinesin-like Protein 2 (TPX2) at Threonine 72 in Spindle Assembly*

Received for publication, July 11, 2014, and in revised form, February 13, 2015 Published, JBC Papers in Press, February 16, 2015, DOI 10.1074/jbc.M114.591545

**Su Yeon Shim[‡], Ignacio Perez de Castro[§], Gernot Neumayer[‡1], Jian Wang[‡], Sang Ki Park[¶], Kamon Sanada[‖], and Minh Dang Nguyen[‡2]**

*From the [‡]Departments of Clinical Neurosciences, Cell Biology & Anatomy, and Biochemistry & Molecular Biology and Hotchkiss Brain Institute, University of Calgary, Calgary, Canada T2N4N1, the [¶]Department of Life Sciences, Pohang University of Science and Technology, Pohang 790-784, Republic of Korea, the [‖]Molecular Genetics Research Laboratory, Graduate School of Science, The University of Tokyo, Hongo 7-3-1, Bunkyo-ku, Tokyo 113-0033, Japan, and the [§]Cell Division and Cancer Group, Centro Nacional de Investigaciones Oncológicas (CNIO), Madrid 28029, Spain*

**Background:** The Targeting protein for *Xenopus* kinesin-like protein 2 (TPX2) is a key factor for spindle assembly; its deregulation is associated with numerous cancers.
**Results:** Phosphorylation of TPX2 at $Thr^{72}$ regulates its spindle assembly functions via Aurora A and Eg5.
**Conclusion:** Proper regulation of TPX2 phosphorylation at $Thr^{72}$ is required for spindle assembly.
**Significance:** Our study provides new mechanistic insights into the spindle and cancers-associated roles of TPX2.

**The human ortholog of the targeting protein for *Xenopus* kinesin-like protein 2 (TPX2) is a cytoskeletal protein that plays a major role in spindle assembly and is required for mitosis. During spindle morphogenesis, TPX2 cooperates with Aurora A kinase and Eg5 kinesin to regulate microtubule organization. TPX2 displays over 40 putative phosphorylation sites identified from various high-throughput proteomic screenings. In this study, we characterize the phosphorylation of threonine 72 ($Thr^{72}$) in human TPX2, a residue highly conserved across species. We find that Cdk1/2 phosphorylate TPX2 *in vitro* and *in vivo*. Using homemade antibodies specific for TPX2 phosphorylated at $Thr^{72}$, we show that this phosphorylation is cell cycle-dependent and peaks at M phase. Endogenous TPX2 phosphorylated at $Thr^{72}$ does not associate with the mitotic spindle. Furthermore, ectopic GFP-TPX2 T72A preferentially concentrates on the spindle, whereas GFP-TPX2 WT distributes to both spindle and cytosol. The T72A mutant also increases the proportion of cells with multipolar spindles phenotype. This effect is associated with increased Aurora A activity and abnormally elongated spindles, indicative of higher Eg5 activity. In summary, we propose that phosphorylation of $Thr^{72}$ regulates TPX2 localization and impacts spindle assembly via Aurora A and Eg5.**

The Targeting protein for *Xenopus* kinesin-like protein 2 (TPX2)[3] is a microtubule (MT)-associated protein critical for spindle morphogenesis (1). This function of TPX2 is consistent with its cell cycle-dependent expression that is lowest during $G_1$ phase and highest during M phase (2). During mitosis, TPX2 associates with MTs and poles of the spindle, where it mediates diverse functions. As indicated by its name, TPX2 localizes Xklp2 to the spindle poles, a key event for spindle bipolarity (1). TPX2 is also required for MT nucleation in the vicinity of chromosomes and MT bundling (3–5). Depletion of TPX2 in HeLa cells significantly decreases chromatin-mediated MTs nucleation without affecting centrosome-mediated MT nucleation, and causes mitotic block (5) as well as multipolar spindles (6). Furthermore, primary cell cultures from a TPX2 knock-out mouse display defects in MTs nucleation around the chromosomes, thereby leading to aberrant spindle formation and chromosome missegregation (7). Similarly, overexpression of TPX2 blocks spindle formation, arrests cells in prometaphase, and causes spindle defects (5, 8).

TPX2 also contributes to MT branching during spindle assembly. In this context, TPX2 cooperates with Augmin to amplify MT mass and preserve MT polarity (9). In addition, TPX2 activates Aurora A, a mitotic kinase important for separation and maturation of centrosomes and for ensuring proper formation of bipolar spindles (for a complete review of the mechanism of action of TPX2 on Aurora A (see Ref. 10)). Interestingly, like TPX2 depletion or overexpression, both inactivation or amplification of Aurora A induces multipolar spindles phenotypes (11–13). Finally, the localization and activity of Eg5, a plus-end directed motor protein that belongs to the Kinesin-5 subclass, is regulated by TPX2 (14). Eg5 affects mitotic spindle organization and spindle assembly by MT cross-linking, sliding along MTs and generating outward forces for spindle pole separation at mitotic entry (14, 15). In mam-

* This work was supported in part by the Canadian Institutes of Health Research (CIHR) (to M. D. N.), Alberta Innovates Health Solutions (AIHS) (to M. D. N.), the Spanish Ministry of Economy and Competitiveness Programa de Acción Estratégica de Salud, 2014, Grant PI14-00227 (to I. P. dC), Framework of International Cooperation Program, managed by National Research Foundation of Korea, Grant 2012K2A1A2033117 (to M. D. N. and S. K. P.), a Grant-in-Aid for Exploratory Research from the Ministry of Education, Culture, Sports, Science and Technology of Japan, and a research grant from Daiichi Sankyo Foundation of Life Science (to K. S.).
[1] Received a DOC scholarship from the Austrian Academy of Science.
[2] Held a Career Development Award from the Human Frontier Science Program Organization, a New Investigator Award from the CIHR, and a Scholar Award from the AIHS. To whom correspondence should be addressed. Tel.: 403-210-5494; Fax: 403-210-8840; E-mail: mdnguyen@ucalgary.ca.

[3] The abbreviations used are: TPX2, Targeting protein for *Xenopus* kinesin-like protein 2; MT, microtubule; Ab, antibody; ANOVA, analysis of variance; IP, immunoprecipitated; Cdk, cyclin-dependent kinase.

malian cells, inhibition of the TPX2/Eg5 association causes alterations in mitotic spindle length/polarity and enhanced MT nucleation around chromosomes (14, 15). In summary, TPX2 promotes spindle assembly and mitosis in human cells through multiple mechanisms.

Although TPX2 contains 747 amino acids that predict a mass of 86 kDa, the observed molecular mass on SDS-PAGE is about 100 kDa. This observation suggests post-translational modifications of the protein (16). PhosphoSitePlus, an online database providing information on protein post-translational modifications shows that TPX2 has over 40 *in vivo* putative phosphorylation sites (17). In *Xenopus* egg extracts, TPX2 is phosphorylated specifically during mitosis and this can be enhanced by taxol-mediated stabilization of mitotic MTs (18). Several putative cdc2 and MAP kinase sites were detected on TPX2 from these extracts using mass spectrometry. Human TPX2 is also phosphorylated during M phase (2). Together, these data indicate that the functions of TPX2 might be regulated by phosphorylation. In particular, numerous high-throughput phosphoproteomic screens and this study identified threonine 72 (Thr$^{72}$), a highly conserved residue among TPX2 species, as a potential phosphorylation site in human cells (19–32). However, this site has never been validated and investigated. Based on the frequent detection of Thr(P)$^{72}$ peptides in phosphoproteome screens (19–32) and our own mass spectrometry of phospho-TPX2 sites, we verified and characterized the phosphorylation of Thr$^{72}$ in cycling cells. We propose that phosphorylation at this residue regulates TPX2 localization and impacts spindle morphogenesis via Aurora A and Eg5.

## EXPERIMENTAL PROCEDURES

*Mass Spectrometry Analysis*—HeLa cells were synchronized using 100 ng/ml of nocodazole for 16 h. After three PBS washings, cells were released into fresh DMEM without nocodazole for 30 min. Cells were harvested and washed with PBS twice before addition of lysis buffer. Protein lysate concentrations were measured using the Bradford protein assay (Bio-Rad). Endogenous TPX2 was immunoprecipitated from 10 mg of total protein lysates using TPX2 Abs (clone 184, Novus Biologicals) and Protein A/G-Sepharose 4 Fast Flow beads. The beads were then washed five times with 500 ml of lysis buffer containing protease inhibitors. The IP samples were run on SDS-PAGE, and Coomassie Blue-stained bands around the expected size of 100 kDa were excised from the gel and sent for mass spectrometry analysis at the University of Victoria Proteomic Center. Another set of IP samples was analyzed by Western blotting using Thr(P)$^{72}$ and pan-TPX2 Abs. Sample preparation for LC-MS/MS analysis was performed at the University of Victoria Proteomic Center. For mass spectrometry data analysis, raw files analyzed with Proteome Discoverer software (Thermo Scientific) were submitted to Mascot 2.2 and compared with *Homo sapiens* of Uniprot-Swissprot, Uniprot Trembl, and IPI human database entries.

*Generation of Phosphospecific Thr$^{72}$ TPX2 Antibodies*—The phosphospecific Abs recognizing phospho-TPX2 at threonine 72 were raised in rabbit against the phosphopeptide (K)LQQAIV(pT*72)PLKPVD that comprises amino acids 66 to 78 of human TPX2. The N-terminal lysine was added to promote solubility. The peptide was conjugated to keyhole limpet hemocyanin (carrier for the phosphopeptide hapten) and was used for immunization of rabbits. The phosphospecific Abs were affinity purified from the antiserum using standard laboratory protocols. Briefly, non-phosphorylated peptide or phosphorylated peptide was coupled to two different agarose columns of SulfoLink® coupling gel using SulfoLink® Immobilization kits (Pierce). Crude serum was first applied to the column coupled with non-phosphorylated peptide, then the flow-through was applied to the column coupled with the phosphorylated peptide. The phosphospecific Abs were eluted from the phosphorylated peptide column.

*In Vitro Cdk Kinase Assay*—*In vitro* kinase assays were performed using active Cdk-cyclin complexes and GST fusion proteins. 10 $\mu$g of GST-TPX2 WT, T72A, and T72E fusion proteins were incubated with 1 $\mu$g of each active Cdk1-cyclin B or Cdk2-cyclin A in the presence of 1 mM ATP (Sigma) at 30 °C for 30 min in kinase buffer (25 mM Tris-HCl (pH 7.5), 5 mM $\beta$-glycerophosphate, 2 mM dithiothreitol (DTT), 0.1 mM $Na_3VO_4$, 10 mM $MgCl_2$, 8 mM MOPS (pH 7.0), 0.2 mM EDTA). As control, 10 $\mu$g of GST-TPX2 protein was incubated with 1 mM ATP in the same condition as above without any active Cdk-cyclin complex. Kinase reactions were stopped by adding 5× SDS-PAGE loading buffer into each sample. Western blot analysis was performed with reaction products using TPX2 (clone 184, Novus Biologicals), Thr(P)$^{72}$, Cdk1, and Cdk2 Abs.

*RNA Interference Sequences*—Two unique TPX2-specific siRNA oligos were used to knock down endogenous TPX2. The first TPX2 siRNA oligo (5′-GAAUGGAACUGGAGGGCUU-3′; called TPX2 cds siRNA in this paper) has been described previously and specificity has been thoroughly demonstrated (5). This TPX2 cds siRNA targets a coding region of human TPX2 (hTPX2) 160–179 bp from the start codon. The second siRNA oligo (5′-AAGGCTAATAATGAGATCTAA-3′; called TPX2 UTR siRNA in this paper) targets a 3′ untranslated region (3′ UTR) of hTPX2 mRNA. This TPX2 UTR siRNA was purchased from Qiagen and was validated previously (33). "All-Stars negative control siRNA" (Qiagen) was used as a negative control.

*Generation of GFP-TPX2 Wild-type and Mutant Constructs*—To generate the GFP-TPX2 wild-type vector, human TPX2 cDNA (bp 3–2241) was cloned into pEGFP-C1 (Clontech). Site-directed mutagenesis was carried out on this plasmid to generate the T72A mutant. GFP-TPX2 T72A was generated by PCR using a mutation primer set (5′ phosphorylated T72A forward primer: CAAGCTATTGTCGCACCTTTGAAACCAG and 5′phosphorylated T72A reverse primer: CTGAAGATT-AGCCTTTCTCAAAGGAG) and Phusion Hot Start DNA Polymerase (Finnzymes) to mutate threonine (ACA) to alanine (GCA). Mutated PCR products were circularized by ligation using a Rapid DNA ligation kit (Thermo Scientific). The mutation was confirmed by DNA sequencing.

*Protein Extraction and Western Blotting*—After PBS washing, cells were lysed in an appropriate volume of mild and non-denaturing lysis buffer (20 mM Tris-HCl (pH 7.5), 150 mM NaCl, 1 mM $Na_2EDTA$, 1 mM EGTA, 1% (v/v) Triton, 2.5 mM sodium pyrophosphate, 1 mM $\beta$-glycerophosphate, 1 mM $Na_3VO_4$, 1 mM phenylmethylsulfonyl fluoride (PMSF), a protease inhibitor

mixture tablet (Roche Applied Science), and 1 mM microcystin-LR (Cayman chemical)). Lysates were incubated on ice for 10 min and sonicated for 5 s twice using a Sonic Dismembrator Model 100 at level 4. Cells were centrifuged for 10 min at 14,000 × *g* to get clear supernatants. Supernatants were collected and protein concentrations were quantified using the Bradford method (Bio-Rad protein assay dye reagent) and bovine serum albumin (BSA, EMD Millipore) as a standard. Proteins in SDS gel-loading buffer (4% (v/v) SDS, 0.2% (v/v) bromphenol blue, 20% (v/v) glycerol, 20 mM β-mercaptoethanol) were run on SDS-PAGE and transferred onto PVDF (polyvinylidene fluoride) membranes for Western blot analysis. After blocking in 5% skim milk solution in PBS-T (1× PBS containing 0.2% Tween 20), each membrane was incubated with specific primary Abs overnight at 4 °C. After washing 3 times using PBS-T for 5 min, membranes were incubated in 5% skim milk in PBS-T containing secondary Abs at 1:5000 dilutions for 1 h at room temperature. After PBS-T washing 3 times each for 5 min, Western Lighting® Enhanced Chemiluminescence solution (PerkinElmer Life Sciences) was added onto membranes for 2 min, and x-ray films (Hyblot CL® autoradiograph film, Denville Scientific, Inc.) were exposed to the membranes. The resulting films were developed using a Kodak X-Omat 2000A processor. To re-probe membranes with other Abs, membranes were incubated in a striping buffer (2% SDS, 62.5 mM Tris (pH 6.8), 100 mM β-mercaptoethanol) for 15 min at 50 °C, washed 3 times with PBS-T, blocked in 5% skim milk in PBS-T, and developed as described above. Results on x-ray films were scanned using a DuoScan T1200 scanner (Agfa). Quantification of each band signal was performed using Quantity One analysis software (Bio-Rad). Signals were normalized to the levels of loading controls (α-actin or non-phosphorylated form of the proteins of interest).

*Immunoprecipitations*—Cells were harvested, lysed, and incubated on ice for 10 min. Cell extracts were sonicated twice for 5 s using a Sonic Dismembrator Model 100 at level 4. After clearance by centrifugation at 16,500 × *g* at 4 °C for 10 min, supernatants were collected for protein quantification. 1 mg of protein of each cell lysate was used for IP. Samples were precleared by incubation with protein A/G-Sepharose for 45 min, and then supernatants were incubated with primary Abs against the target protein for 3 h under gentle rotation at 4 °C. Next, the samples were incubated with protein A/G-Sepharose for an additional hour, continuing rotation at 4 °C. Immunoprecipitates were washed in lysis buffer for 5 min four times, resuspended in SDS gel-loading buffer, and analyzed by Western blotting.

*λ-Protein Phosphatase Treatment*—Immunoprecipitated proteins on beads were washed 4 times with lysis buffer and equally divided into two aliquots. The samples were then washed with 1× λ-protein phosphatase (λ-PPase) buffer (50 mM Tris-HCl, 0.1 mM $Na_2EDTA$, 5 mM DTT, 0.01% (v/v) Brij 35 (pH 7.5)) two times, and treated with or without 400 units of λ-PPase (New England Biolabs) in 1× λ-PPase buffer at 30 °C for 30 min in the presence of 2 mM $MnCl_2$. Reactions were stopped by adding 5× SDS gel-loading buffer.

*Transfection of Cells with Plasmid Constructs and siRNAs*—HeLa and HEK-293 cells (catalog numbers CCL-2 and CRL-1573; American Type Culture Collection (ATCC)) were maintained in high glucose Dulbecco's modified Eagle's medium (DMEM) containing 10% fetal bovine serum (FBS) and 1% penicillin/streptomycin (all from Gibco). For transient transfection with single siRNA, cells were seeded on 60-mm cell culture dishes shortly before transfection. siRNA transfection was performed using HiPerFect transfection reagent (Qiagen) according to the manufacturer's protocol using 20 nM siRNA and 20 μl of HiPerFect reagent for each dish. Transient transfection of cells with plasmid DNAs alone or co-transfection of siRNA with plasmids was performed using Lipofectamine™ 2000 (Invitrogen). Cells were seeded on 60-mm cell culture dishes 1 day before transfection. Cells were transfected according to the manufacturer's recommended protocol using 3 μg of plasmids with 10 μl of Lipofectamine 2000 transfection reagent or 20 nM siRNA oligos and 3 μg of plasmids with 10 μl of Lipofectamine 2000 transfection reagent for each dish.

*Cell Cycle Synchronization*—HeLa cells were synchronized at S phase by double thymidine block. Cells were treated with 2 mM thymidine for 18 h, followed by 8 h of release in fresh DMEM, and then, re-treated with thymidine for 18 h. For M phase, cells were synchronized using nocodazole treatment. For un-transfected cells, 3–5 h after seeding, cells were treated with 100 ng/ml of nocodazole (Sigma) for 16–17 h, followed by PBS washes twice and incubation in fresh DMEM for 30 min. For synchronization of plasmid-transfected cells at M phase, 24–29 h after transfection, cells were changed into fresh DMEM containing 100 ng/ml of nocodazole (Sigma), and incubated for 16–17 h. Cells were then washed twice in PBS and incubated in fresh DMEM for 30 min. The different cell cycle stages were confirmed by flow cytometry analysis.

*Flow Cytometry Analysis*—After transfection, with or without synchronization, cells were harvested with trypsin/EDTA (0.25%, Invitrogen), washed twice with PBS, re-suspended in 500 μl of PBS, and then fixed with 500 μl of ethanol for at least 24 h. After centrifugation at 2,095 × *g* for 10 min, the cell pellets were re-suspended in a mixture of 500 μl of PBS and 500 μl of propidium iodide solution (Molecular Probes) containing ribonuclease A (RNase A, Sigma) and Triton X-100 (Fisher Scientific). The prepared samples were sent to the Flow Cytometry Core Facility (University of Calgary) for cell cycle profiling using a BD Biosciences FACScan flow cytometer.

*Treatment with CDK Inhibitors*—HeLa cells were seeded on 100-mm cell culture dishes at a density of $2 \times 10^6$ cells per dish. 3 h after seeding, cells were treated with 100 ng/ml of nocodazole for 16 h. Mitotic cells were incubated with dimethyl sulfoxide (as a vehicle control), 20 or 40 mM drugs (roscovitine or alsterpaullone) for 30 min in the presence of nocodazole in the medium. After treatment, cells were trypsinized, and washed twice in PBS. After centrifugation, cell pellets were dissolved in lysis buffer containing protease inhibitor mixture tablets (Roche) and 1 μM microcystin-LR (Cayman Chemical). The prepared cell lysates were used for IP experiments. CDK inhibitor experiments were performed in triplicate.

*Antibodies*—Primary Abs against Cdk1, Cdk2 (Santa Cruz), Thr(P)$^{72}$ TPX2 (homemade, described above), Cyclin B (Abcam),

α-actin (Chemicon), TPX2 (clone 183, epitope: 150–200 amino acids of human TPX2, Novus Biologicals; clone 184, epitope: 700–749 amino acids of TPX2, Novus Biologicals), phospho-Cdk/MAPK substrates (34B2, Cell Signaling), Cy3 conjugated-β-tubulin (Sigma), p-Aurora A (ab18318, Abcam), and monoclonal TPX2 (18D5-1, Abcam) were used for Western blots, immunoprecipitations, and/or immunofluorescence experiments. Donkey anti-rabbit IgG HRP and sheep anti-mouse IgG HRP from GE Healthcare were used as secondary Abs for Western blots. For immunofluorescent staining, Cy3- and FITC-conjugated anti-mouse IgG or anti-rabbit IgG (Jackson ImmunoResearch) were used.

*Quantification of the Cells with Monopolar, Bipolar, and Multipolar Mitotic Spindles*—HeLa cells were seeded on glass coverslips at a density of $5 \times 10^4$ cells/well in 24-well cell culture plates. The next day, cells were transfected with 1 μg of each plasmid (GFP, GFP-TPX2 WT, or GFP-TPX2 T72A). 24 h after transfection, cells were synchronized with nocodazole (100 ng/ml) for 16 h. Cells were then released from the nocodazole block by washing three times in PBS and incubated in fresh medium for 30 min. Cells were fixed with 4% PFA and stained with Cy3-conjugated β-tubulin antibody for mitotic spindle visualization. Samples were observed under a fluorescence microscope and GFP-positive (transfected) cells in prometaphase or metaphase were categorized into three different classes based on the number of spindle poles: monopolar, bipolar, and multipolar spindles. Over 100 prometaphase or metaphase cells were scored per slide and five separate slides were examined for condition. The percentages of cells in each experimental group were calculated. The differences in the mean values for each group were analyzed by ANOVA. In a separate experiment, HeLa cells were seeded on glass coverslips in 24-well cell culture plates ($5 \times 10^4$ cells/well). The next day, 20 pmol of TPX2 UTR siRNA duplexes (to deplete endogenous TPX2) were co-transfected with 500 ng of each plasmid (an empty GFP vector, GFP-TPX2 WT, or GFP-TPX2 T72A) into cells using 2 μl of Lipofectamine 2000 (Invitrogen) according to the manufacturer's protocol. 24 h after transfection, cells were synchronized with nocodazole (100 ng/ml) for 16 h. Cells were then washed 3 times in PBS and released into fresh medium for 30 min. Fixation and quantification were performed exactly as described above.

*Immunofluorescent Staining, Signal Quantification, and Confocal Microscopy Analysis*—Cells on coverslips were fixed with 4% PFA (4% paraformaldehyde in 1× PBS (pH 7.4)) for 10 min at 37 °C. Fixed cells were washed with PBS twice and blocked in blocking buffer (3% BSA, 0.2% Triton-X 100 in 1× PBS) for 1 h at room temperature. Next, coverslips were incubated with primary Abs in blocking buffer overnight at 4 °C. After washes in PBS, coverslips were incubated with secondary Abs conjugated with Cy3 or FITC (Jackson ImmunoResearch), followed by DAPI staining for DNA visualization. After three washes in 1× PBS, cells on coverslips were mounted on microslides (VWR international) using a drop of Aqua-Mount (Thermo Scientific). Images were acquired by a Nikon D-Eclipse C1 confocal microscope with its EZ-C1 software. For the quantitative analysis of exogenous EGFP-TPX2, Thr(P)$^{288}$ Aurora A, and α-Tubulin immunofluorescent signals, acquired images were processed and analyzed using Adobe Photoshop CS8.0 and ImageJ-win64. Integrated intensity was calculated at the cellular level and/or at specific subcellular locations. Spindle length was determined using ImageJ by calculating the distance between spindle poles inferred from the EGFP-TPX2 signals.

*Blocking Peptide Experiments*—The sequence of the blocking peptide is LQQAIVTPLKPVD (from 66 to 78 amino acids of human TPX2) and is exactly the same sequence used to generate the phosphospecific TPX2 Abs at Thr$^{72}$. The threonine amino acid has been phosphorylated. The generation and purification of the blocking peptide was performed at the University of Calgary peptide service facility. The peptide was synthesized on preparative HPLC (a Waters HPLC system) using a Vydac C18 column. Phosphothreonine peptide modification was carried out using standard *N*-(9-fluorenyl)methoxycarbonyl chemistry (*N*-α-(9-fluorenyl)methoxycarbonyl-*O*-benzyl-L-phosphothreonine derivative reagent was used to prepare this phosphothreonine peptide). The quality of the peptide was evaluated by analytical HPLC and mass spectrometry. Purity assessment by analytical HPLC showed a single peak representing almost 100% purity of this peptide (the assessment was performed by the University of Calgary peptide service facility). For the blocking experiments, the Abs were combined with a 5-, 10-, 20-, and 50-fold excess of blocking peptide and preincubated at 4 °C overnight.

*Statistical Analysis*—Data analysis to determine *p* values was performed using an unpaired Student's *t* test when comparing two groups, or ANOVA for comparing multiple groups. *p* values of $<0.05$ were considered statistically significant in both unpaired Student's *t* test and ANOVA. The Newman-Keuls test was performed when difference between multiple groups was revealed by ANOVA (significant *p* values).

## RESULTS

*Cdk1 and Cdk2 Phosphorylate TPX2 in Vitro*—Thr$^{72}$ is a highly conserved residue among human, mouse, rat, and frog TPX2 (Fig. 1*A*). This residue is one of the uncharacterized TPX2 phosphorylation sites that commonly appear in several human phosphoproteome studies (19–32). It lies within a consensus sequence recognized by Cdk1, Cdk2, and Cdk5, an atypical Cdk active in post-mitotic cells (34). Consistent with previous studies (19–32), we also detected phosphorylation of Thr$^{72}$ in synchronized mitotic HeLa cells using mass spectrometry. Indeed, following immunoprecipitation with pan-TPX2 Abs from mitotic HeLa cell lysates, the existence of phospho-Thr$^{72}$ (Thr(P)$^{72}$) TPX2 was confirmed by identification of Thr(P)$^{72}$ peptides by LC-MS/MS analysis (Fig. 1*B*). 14 additional putative phosphorylation sites identified in previous studies (17, 19–32) were also found in our analysis (Fig. 1*C*). We first generated polyclonal antibodies specific to Thr(P)$^{72}$ TPX2 (Thr(P)$^{72}$ TPX2 Abs, see "Experimental Procedures"). We then performed *in vitro* phosphorylation assays of GST-TPX2 fusion proteins with or without mutation at Thr$^{72}$ (GST-TPX2, GST-TPX2 T72A, and GST-TPX2 T72E) using active Cdk1-cyclin B and Cdk2-cyclin A. The purposes of these experiments were to determine whether Thr$^{72}$ can be phosphorylated by Cdk1/2 and to test the specificity of the phospho-Abs

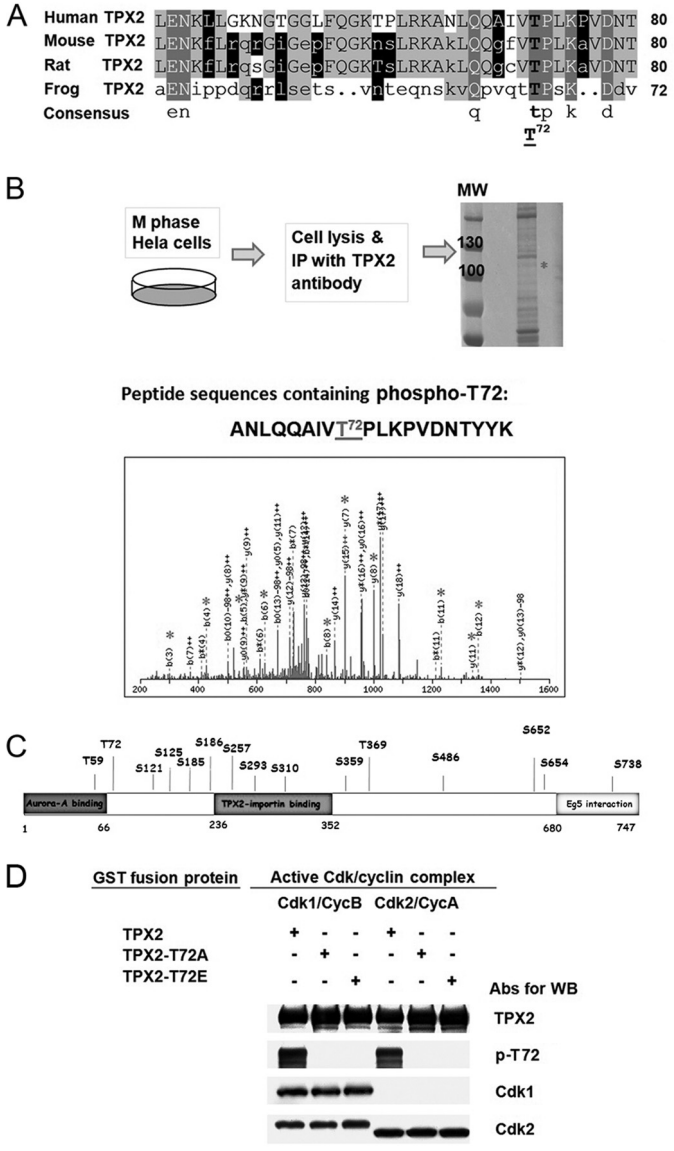


FIGURE 1. **The evolutionary conserved Thr$^{72}$ in human TPX2 is phosphorylated by Cdk1 and Cdk2 *in vitro*.** *A*, comparative alignment of part of human TPX2 sequence (amino acids 41 to 80) with corresponding sequences from other species (mouse, rat, and frog) using DNAMAN software (Lynnon Corporation). The sequence alignment shows that Thr$^{72}$ in human TPX2 is conserved in all other species. *B*, schematic diagram of the experimental protocol for mass spectrometry analysis (LC-MS/MS) using mitotic HeLa cells. HeLa cells were synchronized at M phase by nocodazole treatment (100 ng/ml) for 16 h and released for 30 min after nocodazole washout. Endogenous TPX2 was immunoprecipitated from 10 mg of total protein using pan-TPX2 Abs (clone 184). IP sample was run on SDS-PAGE and after Coomassie Blue staining, the band with the matching size to TPX2 (confirmed by Western blotting with TPX2 Abs, not shown) was cut out and sent for LC-MS/MS analysis. The *gray asterisk* on the spectra of the phosphopeptide containing Thr$^{72}$ indicate the identified matched fragment ions on mass spectrometry. *C*, phosphorylation sites identified by mass spectrometry analysis on endogenous TPX2 immunoprecipitated from nocodazole-synchronized mitotic HeLa cells in regards to the known TPX2 domains. All these sites have been identified previously (17, 19–32) but not confirmed and analyzed. Thr$^{72}$ is the first validated and functionally characterized phosphorylation site in human TPX2 (this study). *D, in vitro* kinase assay using purified Cdk1/2 proteins and phosphospecific Thr$^{72}$ TPX2 Abs. Purified GST fusion protein TPX2 WT, GST-TPX2-T72A, or GST-TPX2-T72E was incubated with each active Cdk-cyclin complex in the presence of 1 mM cold ATP. All kinase reactions were stopped by adding 2× SDS sample buffer and the samples were run on SDS-polyacrylamide gel electrophoresis followed by Western blot detection using the indicated antibodies.

*in vitro*. Using our homemade Thr(P)$^{72}$ TPX2 Abs, we found that GST-TPX2 is phosphorylated at Thr$^{72}$ *in vitro* by Cdk1-cyclin B and Cdk2-cyclin A (Fig. 1*D*). In addition, our *in vitro* kinase assays revealed that the Thr(P)$^{72}$ TPX2 Abs only recognized purified wild-type TPX2 protein phosphorylated by Cdk1/2 *in vitro* but not the mutated GST-TPX2 T72A and GST-TPX2 T72E that cannot be phosphorylated (Fig. 1*D*). Taken together, our results indicate that TPX2 is phosphorylated *in vitro* at Thr$^{72}$ by Cdk1 and Cdk2. Also, our homemade Thr(P)$^{72}$ TPX2 Abs are specific to TPX2 phosphorylated at Thr$^{72}$ *in vitro*.

*In Vivo Specificity of the Thr(P)$^{72}$ TPX2 Antibodies*—TPX2 is phosphorylated at Thr$^{72}$ by the mitotic Cdk1-cyclin B complex *in vitro* (Fig. 1*D*) and Thr(P)$^{72}$ TPX2 peptides are detected in human cell lysates (including HeLa cells) by mass spectrometry (Fig. 1*B* and Refs. 19–32). Thus, TPX2 phosphorylation at Thr$^{72}$ may occur during mitosis. For these reasons, we employed mitotic HeLa cells (a cell line that has been thoroughly used for the study of TPX2 (5, 8, 33, 35–37)) to determine the specificity of the Thr(P)$^{72}$ TPX2 Abs *in vivo*. HeLa cells were transiently transfected with control siRNA or two specific TPX2 siRNAs (siRNA #1 and #2, see Refs. 33 and 36 and "Experimental Procedures" for details and specificity of the siRNAs) for 24 h, synchronized at M phase for 16 h, and then lysed for Western blots. The intensity of the TPX2 major band was significantly decreased by 67 and 70%, respectively, in samples treated with TPX2 siRNA #1 and #2 when compared with control siRNA-treated samples (Fig. 2, *A* and *B*). Stripping of the blots and re-development with pan-TPX2 Abs confirmed that Thr(P)$^{72}$ TPX2 Abs recognize TPX2 from mitotic HeLa cells (Fig. 2, *A* and *B*). To test whether Thr(P)$^{72}$ TPX2 Abs recognize the Thr$^{72}$-phosphorylated form of TPX2 in HeLa cells, we transfected the cells with GFP-TPX2 WT or T72A. 24 h after transfection, we synchronized the cells at M phase with nocodazole for 16 h prior to immunoprecipitation experiments (Fig. 2*C*). One would expect that Thr(P)$^{72}$ TPX2 Abs only recognize the immunoprecipitated phosphorylated form of wild-type TPX2 but not the T72A. We found that both endogenous TPX2 and exogenous GFP-TPX2 fusion proteins were immunoprecipitated with pan-TPX2 Abs. Importantly, Thr(P)$^{72}$ TPX2 Abs only recognize immunoprecipitated exogenous TPX2 from GFP-TPX2 WT-transfected cells, but not from GFP-TPX2 T72A-transfected cells (Fig. 2*C*). Similarly, endogenous TPX2 was detected with Thr(P)$^{72}$ TPX2 Abs (Fig. 2*C*). Treatment of samples with λ-protein phosphatase abolished the Thr(P)$^{72}$ TPX2 Abs signals (Fig. 2*C*). Taken together, our results indicate that Thr(P)$^{72}$ TPX2 Abs are specific to TPX2 phosphorylated at Thr$^{72}$ *in vivo*.

*TPX2 Phosphorylation at Thr$^{72}$ Peaks at Mitosis in HeLa Cells*—Because the expression of TPX2 is cell cycle-dependent, we next asked whether Thr$^{72}$ phosphorylation is regulated during cell cycle. For this experiment, HeLa cells were synchronized at M phase by nocodazole block and, for comparison, at S phase by double thymidine block. Cell cycle profiling confirmed the enrichment at S and M phases (Fig. 3*A*). Endogenous TPX2 was then immunoprecipitated with pan-TPX2 Abs from lysates of non-synchronized cells and cell synchronized at S or M phase prior to Western blots with Thr(P)$^{72}$ TPX2 and pan-

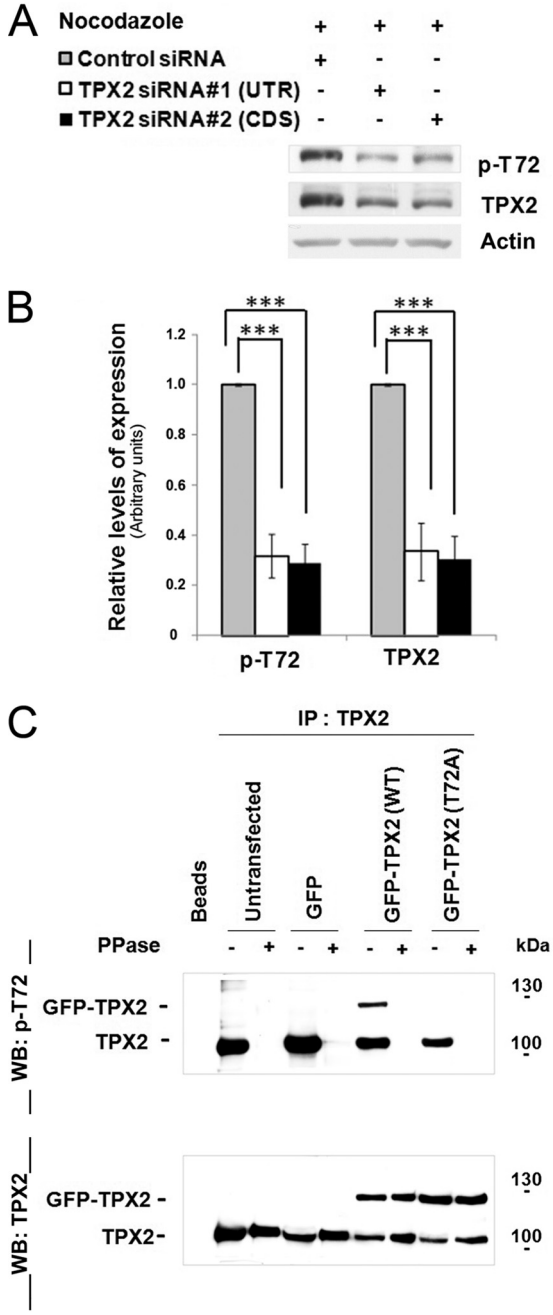


FIGURE 2. **Thr(P)$^{72}$ TPX2 antibodies are specific in Western blot for TPX2 phosphorylated at Thr$^{72}$ *in vivo*.** *A,* specificity of Thr(P)$^{72}$ TPX2 for TPX2 protein tested by siRNA. HeLa cells were transfected with control siRNA or one of two TPX2 siRNAs for 24 h and synchronized at M phase with nocodazole treatment (100 ng/ml). Cells were harvested and lysed with lysis buffer. Samples were run on SDS-PAGE, followed by Western blotting, first probed with the Thr(P)$^{72}$ TPX2 Abs, then stripped and re-probed with pan-TPX2 (clone 184) Abs. Levels of actin were used as loading controls. *B,* bar graph quantitation for the relative expression levels of Thr(P)$^{72}$ TPX2 and TPX2 in control and TPX2 siRNA-transfected cells. Each sample was compared with sample treated with control siRNA. Relative expression levels of Thr(P)$^{72}$ for control siRNA, 1 ± 0; TPX2 siRNA #1 (UTR), 0.318 ± 0.085; TPX2 siRNA #2 (Cds), 0.289 ± 0.115. Relative expression levels of TPX2, control siRNA, 1 ± 0; TPX2 siRNA #1, 0.335 ± 0.0074; TPX2 siRNA #2, 0.304 ± 0.091 (mean ± S.E.). $n = 4$ samples, from 4 independent experiments. Unpaired Student's *t* test indicated all the results are significant. ***, $p < 0.001$. *C,* specificity of Thr(P)$^{72}$ TPX2 tested by the use of T72A mutant and λ-PPase treatment. HeLa cells were left untransfected, transfected with an empty GFP vector, GFP-TPX2 WT, or GFP-TPX2 T72A mutant plasmids. 24 h after transfection, cells were synchronized with nocodazole for 16 h, harvested, and lysed. TPX2 immunoprecipitation was performed in each sample with TPX2 Abs (clone 183). Where indicated, IP beads were treated with λ-PPase before SDS-PAGE. The blot was first probed with the Thr(P)$^{72}$ TPX2 Abs. After stripping, the same blot was re-probed with pan-TPX2 Abs (clone 184).

TPX2 Abs (Fig. 3*B*). As shown in Fig. 3*C*, the levels of Thr(P)$^{72}$ TPX2 are much higher in M phase cells compared with S phase or non-synchronized cells. When the ratio Thr(P)$^{72}$ TPX2/TPX2 levels in non-synchronized cells was set at 1, the relative levels of Thr(P)$^{72}$ TPX2 in M phase cells were ~3–4-fold higher than those found for non-synchronized cells and S phase cells (Fig. 3*C*). In summary, using our homemade Thr(P)$^{72}$ Abs, we demonstrate that TPX2 is phosphorylated at Thr$^{72}$ *in vivo* in a cell cycle-dependent manner, and this phosphorylation peaks at M phase.

*TPX2 Is Phosphorylated in Vivo at Thr$^{72}$ by Cdk1/2*—Thr$^{72}$ was identified as a potential Cdk2 substrate from a mass spectrometry screen using 293 cell lysates (24). Our results showed that TPX2 is phosphorylated at Thr$^{72}$ by Cdk1 and Cdk2 *in vitro* (Fig. 1*D*). In light of these findings, we sought to determine whether TPX2 is also phosphorylated at Thr$^{72}$ by Cdk1 and Cdk2 *in vivo*. To test this, we treated HeLa cells with roscovitine, a purine analog and well known inhibitor of the kinase activity of Cdk1-cyclin B, Cdk2-cyclin A, and Cdk5/p35/p39/p25 (38–40). Roscovitine does not target Cdk5 in HeLa cells because of the absence of Cdk5 co-activators p25, p35, and p39 (41–43). Because Thr$^{72}$ phosphorylation is highest at M phase of the cell cycle (Fig. 3), we performed roscovitine treatment on mitotic cells. HeLa cells were first synchronized with nocodazole at M phase and then treated with two different concentrations of roscovitine (20 and 40 μM) for 30 min in the presence of nocodazole to avoid premature exit from mitosis (44). Upon treatment with roscovitine, the levels of Thr$^{72}$ phosphorylation significantly decreased when compared with levels in mitotic cells treated with dimethyl sulfoxide as a control (Fig. 4*A*). To monitor the efficacy of the treatment, we probed the blots with commercial Abs that recognize phosphorylated proteins containing P*X*(S*/T*)P or (S*/T*)P*X*(R/K) motif (S*, a phosphoserine; T*, a phosphothreonine), often found in Cdk/MAPK substrates. The intensities of the bands detected by these Abs in samples derived from mitotic cells treated with roscovitine were significantly decreased when compared with samples treated with dimethyl sulfoxide (Fig. 4*B*). Importantly, no changes in the levels of cyclin B1 or TPX2 were found in the roscovitine-treated cells, indicating that they had remained in mitosis (Fig. 4*B*). Taken together, our results indicate that roscovitine treatments worked well and that Thr$^{72}$ phosphorylation in HeLa cells can be attenuated by Cdk1/2 inhibition.

*Intracellular Localization of TPX2 Phosphorylated at Thr$^{72}$ in HeLa Cells*—In interphase, TPX2 is predominantly localized in the nucleus (2, 5). During mitosis, TPX2 decorates the mitotic spindle apparatus (2, 5). Phosphorylation of TPX2 at Thr$^{72}$ can possibly dictate its subcellular localization. Using immunofluorescence staining and confocal microscopy, we next determined the subcellular distribution of Thr(P)$^{72}$ TPX2 in interphase and mitotic cells. We first tested the specificity of our Thr(P)$^{72}$ TPX2 Abs for immunostaining using antigen preabsorption with the corresponding blocking peptide (residues 66 to 78, LQQAIVpT$^{72}$PLKPVD). As shown in Fig. 5, following

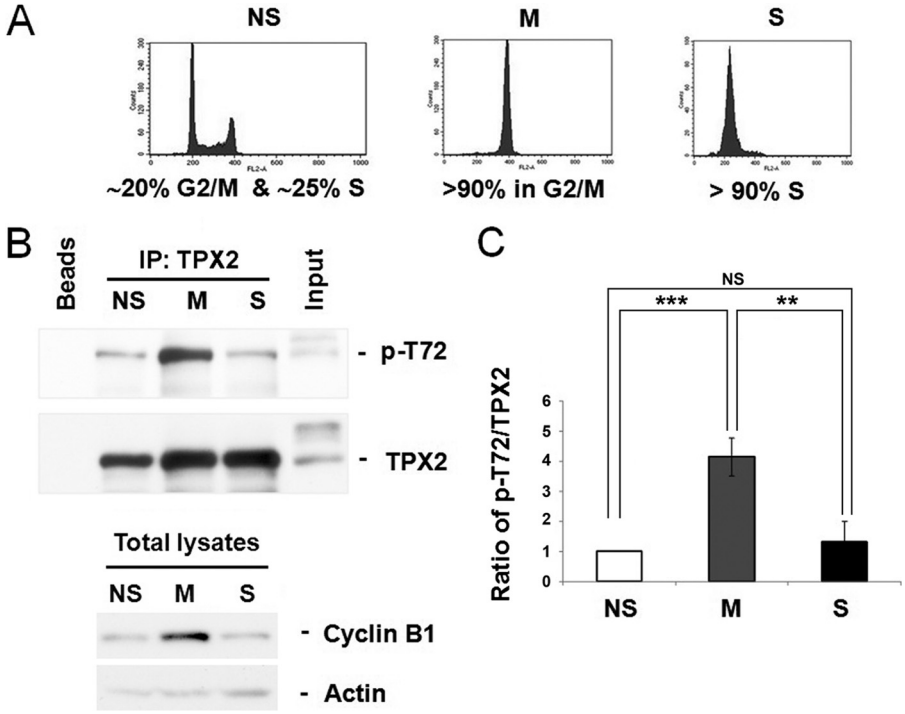


FIGURE 3. ***In vivo* TPX2 phosphorylation at Thr$^{72}$ is cell cycle-dependent and peaks at M phase.** *A,* cell cycle profiles analyzed by flow cytometry analysis to confirm cell synchronization at each phase. *B*, after IPs with pan-TPX2 Abs (clone 184), Western blots were probed first with the Thr(P)$^{72}$ TPX2 Abs and then, after stripping, re-probed with pan-TPX2 Abs (clone 184). The levels of $\alpha$-actin were used as loading controls. The levels of cyclin B1 were used as positive controls to show that synchronization at M phase worked well, as indicated by the high level of cyclin B1 in M phase compared with that of S phase or non-synchronized cells. The Western blot figures are representative of 3 independent experiments. The input blot is from the mitotic samples. *C*, bar graphs for quantification of relative levels of Thr$^{72}$ phosphorylation are shown. *Non-syn*, non-synchronized cells (1 $\pm$ 0); *M*, M phase cells (4.16 $\pm$ 0.36); *S*, S phase cells (1.31 $\pm$ 0.4); mean of the relative levels of Thr(P)$^{72}$ TPX2/TPX2 expression $\pm$ S.D., $n = 3$ independent experiments; ***, non-syn *versus* M phase, $p < 0.001$; **, M *versus* S phase, $p < 0.01$; *NS*, not significant: non-syn *versus* S phase, all by unpaired Student's *t* test.

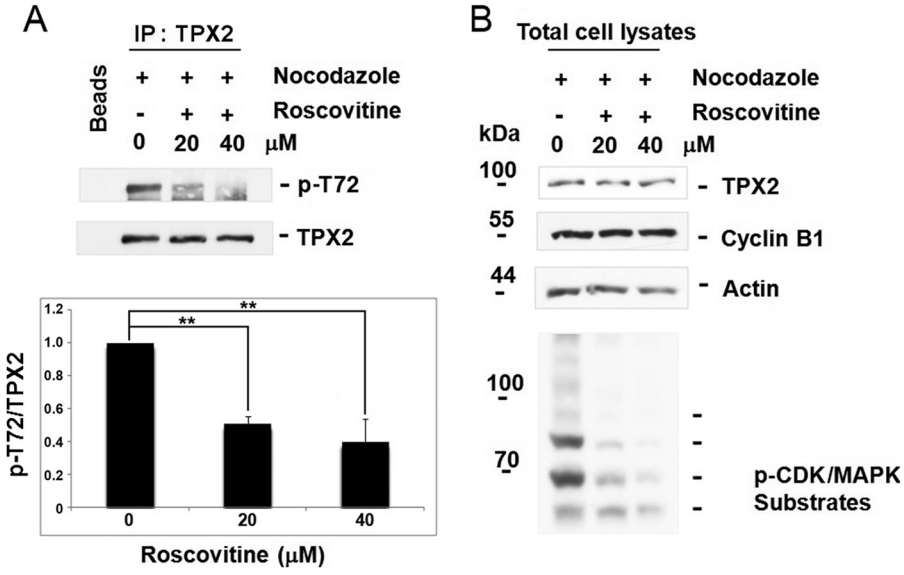


FIGURE 4. **Phosphorylation of TPX2 at Thr$^{72}$ is inhibited by the Cdk inhibitor roscovitine.** *A,* the levels of Thr(P)$^{72}$ were reduced by roscovitine treatment. HeLa cells were first treated with 100 ng/ml of nocodazole for 16 h and then once synchronized, treated with dimethyl sulfoxide (as a control), or 20 and 40 $\mu$M roscovitine for 30 min. Cells were harvested, lysed, and TPX2 was immunoprecipitated with pan-TPX2 Abs (clone 184). SDS-PAGE was performed and followed by Western blotting with Thr(P)$^{72}$ and pan-TPX2 Abs (clone 184). *B,* cyclin B1 levels were also used to confirm that roscovitine-treated cells had remained in mitosis. The levels of p-Cdk/MAPK substrates (P*X*(S*/T*)P or (S*/T*)P*X*(R/K) motif) were also used to confirm the effectiveness of the treatment. Actin levels were used as loading control.

the incubation with the blocking peptide, the Thr(P)$^{72}$ TPX2 immunofluorescent signal was significantly diminished in both mitotic and interphase cells. In contrast, the pan-TPX2 signal remained intact. In interphase cells, Thr(P)$^{72}$ TPX2 is expressed at low levels and is localized in the nucleus (Fig. 5*C*). This is the same localization pattern reported with pan-TPX2 Abs (10, 33, 36). Conversely, during mitosis Thr(P)$^{72}$ TPX2 is predominantly localized in the cytosol (Fig. 5, *A* and *B*). In

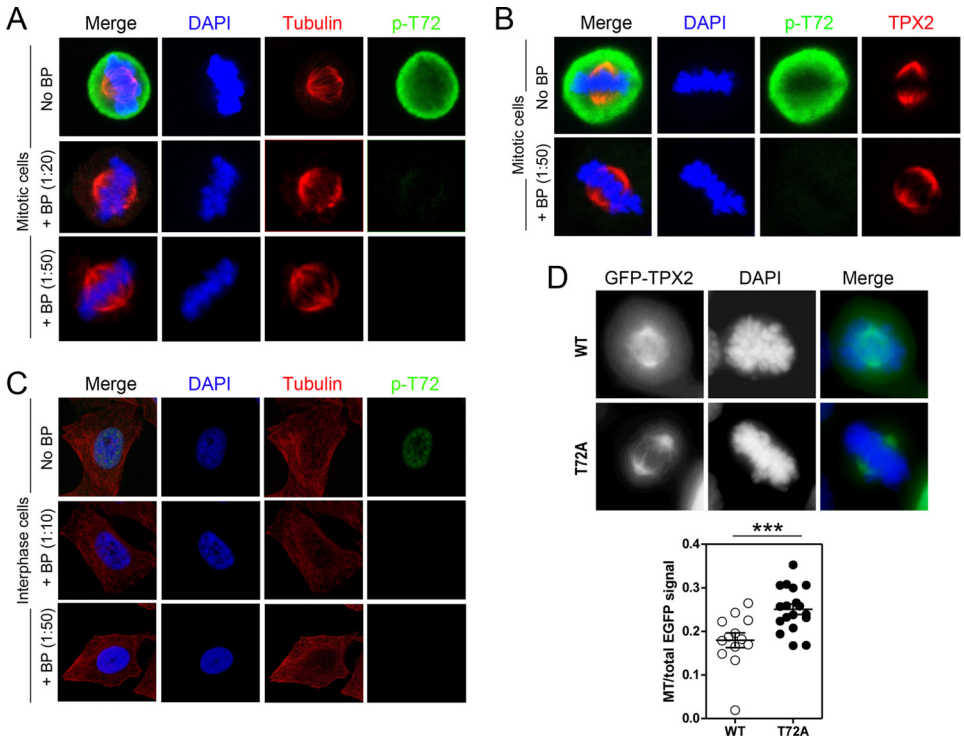


FIGURE 5. **Localization of Thr(P)$^{72}$ TPX2 in HeLa and 293 cells.** Mitotic (*A* and *B*) and interphase (*C*) HeLa cells were stained with Abs directed against Thr(P)$^{72}$ TPX2, TPX2, and tubulin or with the Thr(P)$^{72}$ Abs pre-absorbed with blocking peptide at different ratios. *A,* in mitotic cells, TPX2 phosphorylated at Thr$^{72}$ is localized in the cytosol and does not strictly associate with the mitotic spindle. *B*, HeLa cells stained with pan-TPX2 and Thr(P)72 TPX2 Abs preincubated with Thr(P)72 blocking peptides. *C,* during interphase, Thr(P)$^{72}$ TPX2 is localized in the nucleus. Note that the expression levels of Thr(P)$^{72}$ are much lower in interphase cells than in mitotic cells. Note that only the Thr(P)$^{72}$ signal was blocked. *D,* representative photographs of mitotic 293 cells transfected with GFP-TPX2 WT (WT) and GFP-TPX2 T72A (T72A). Scatter plots show the GFP signal at microtubules relative to total GFP signal. GFP-TPX2 T72A is significantly enriched on microtubules when compared with GFP-TPX2 WT (GFP-TPX2 WT (0.26 ± 0.01, $n = 29$) *versus* GFP-TPX2 T72A (0.39 ± 0.02, $n = 22$), group (mean ± S.E.); ***, $p < 0.0001$ by *t* test). *Scale bar*, 10 $\mu$m.

agreement with the Western blot results on synchronized cells (Fig. 3), levels of Thr(P)$^{72}$ TPX2 were much higher in mitotic cells than in interphase cells (Fig. 5).

To confirm the localization pattern of Thr(P)$^{72}$ TPX2 detected with our homemade Abs, we next expressed at low levels GFP-TPX2 WT and T72A in HEK-293 cells and assessed their distribution during spindle assembly. As shown in Fig. 5*D*, GFP-TPX2 T72A was preferentially localized to the spindle, whereas the GFP-TPX2 WT was found both on the spindle and cytosol. The absence of GFP-TPX2 T72A in the cytosol is not due to a weaker expression when compared with the expression of GFP-TPX2 WT (see Fig. 6). A significant difference in the ratio spindle MTs-associated signal/total signal was observed between WT and T72A (Fig. 5*D*). Together with the use of blocking peptides, the correlation between the localization of endogenous Thr(P)$^{72}$ TPX2 and exogenous TPX2 proteins confirms the specificity of our Thr(P)$^{72}$ TPX2 Ab for immunostaining. In brief, our results indicate that phosphorylation of Thr$^{72}$ regulates the localization of TPX2 during mitosis. Inability to phosphorylate TPX2 at Thr$^{72}$ impairs its distribution to the cytosol and accumulates the protein on the spindle.

*Phosphorylation of TPX2 at Thr$^{72}$ Impacts the Number of Mitotic Spindle Poles* —Because TPX2 plays a key role in spindle assembly and Thr$^{72}$ phosphorylation of TPX2 peaks at M phase (Fig. 3), we next asked whether Thr$^{72}$ phosphorylation regulates the mitotic functions of TPX2. To do so, we examined the effects of GFP-TPX2 WT and GFP-TPX2 T72A on spindle morphology. We first assessed the number of spindle poles in HeLa cells. Cells in prometaphase and metaphase with mitotic spindles were categorized into three different classes based on the number of spindle poles: monopolar, bipolar, and multipolar spindles (more than 2 poles) (see Fig. 6*A* for representative examples). A previous study has shown that GFP-TPX2 overexpression can generate cells with monopolar spindle, cells with bipolar spindles undergoing normal cell cycle without any problem, as well as cells with multipolar spindles (5). Among these cells overexpressing GFP-TPX2, ~60% showed markedly altered morphologies (including apoptotic features), ~35% were in interphase and ~6% were arrested in mitosis (5). In our synchronized cell cultures GFP-TPX2 WT overexpression induced monopolar spindle in ~30% of cells and multipolar spindles in ~3% of cells at the detriment of cells with bipolar spindle when compared with GFP overexpression (Fig. 6*C*). Interestingly, GFP-TPX2 T72A mutant significantly increased the proportion of mitotic cells with multipolar spindles by 9 and 12% when compared with cells transfected with GFP-TPX2 WT or GFP, respectively (Fig. 6*C*). The expression levels of GFP-TPX2 WT and GFP-TPX2 T72A were similar and thus, the results cannot be attributed to the levels of expression but rather to the phosphorylation status of Thr$^{72}$ (Fig. 6*B*).

To ascertain the effects of GFP-TPX2 T72A in the multipolar spindles phenotype, we directly assessed the impact of GFP-TPX2 T72A in cells with depletion of endogenous TPX2. We used specific TPX2 UTR-targeting siRNA to partially knock-

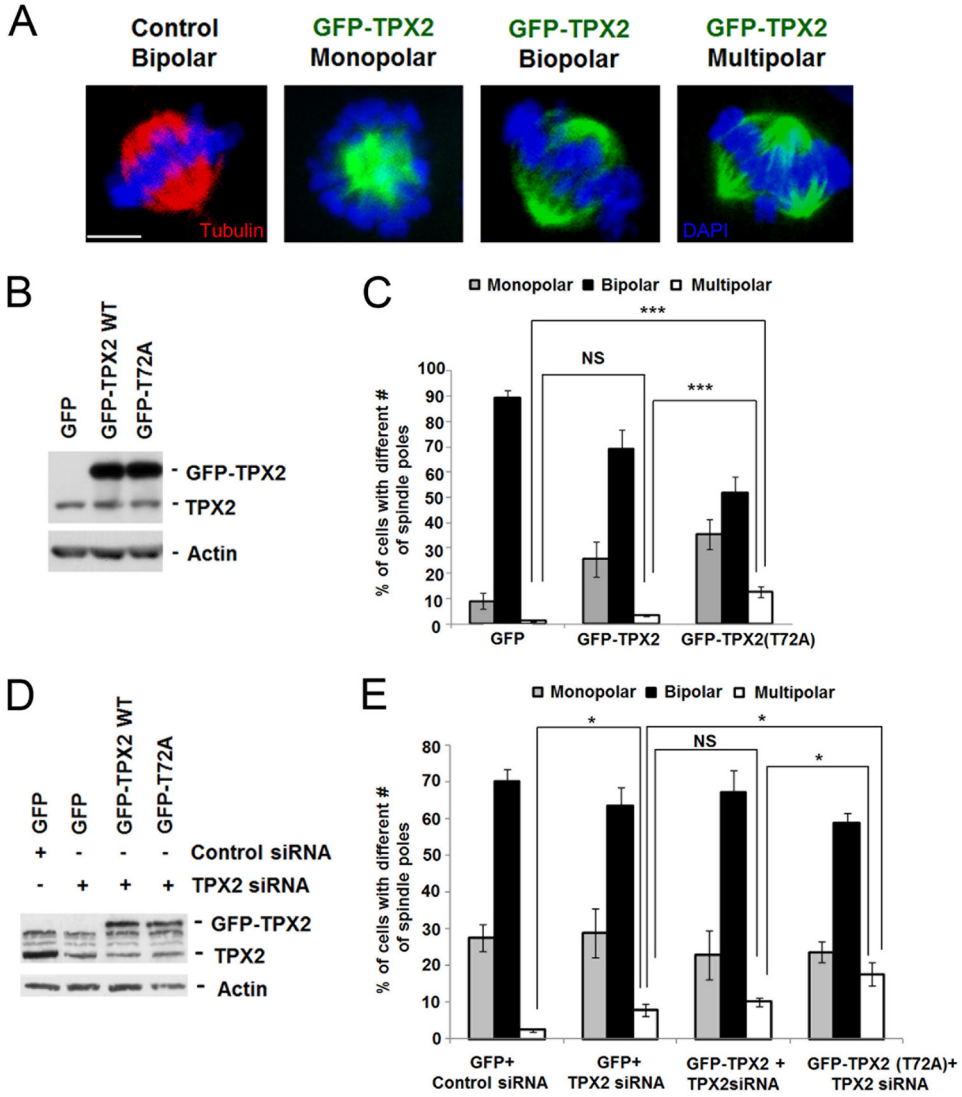


FIGURE 6. **Effects of GFP-TPX2 T72A on the polarity of mitotic spindles in HeLa cells with or without endogenous TPX2.** *A,* representative photographs of mitotic HeLa cells at prometaphase and metaphase with monopolar, bipolar, and multipolar mitotic spindle poles. *Scale bar*, 10 $\mu$m. *B,* Western blots showing the levels of endogenous TPX2, GFP-TPX2 WT, and GFP-TPX2 T72A in cells with intact levels of TPX2. *C, bar graphs* showing the number of cells with different mono-, bi-, or multipolar mitotic spindles in each group. Cells with mitotic spindles were fixed and stained with Cy3-conjugated tubulin for MT visualization. GFP-TPX2 T72A expression results in a significant increase in the percentage of cells with multipolar spindles in the presence of endogenous TPX2. ANOVA comparing the three groups shows high significance with $p < 0.001$. Neuman-Keuls test was used to compare each group: GFP (1.49 $\pm$ 0.47) *versus* T72A (12.72 $\pm$ 2.10), $p < 0.001$; TPX2 WT (3.36 $\pm$ 0.40) *versus* T72A (12.72 $\pm$ 2.10), $p < 0.001$; group (mean $\pm$ S.E.); ***, $p < 0.001$; *NS*, not significant (GFP *versus* TPX2). At least 100 cells for each set of experiments were used for quantification, 5 independent experiments were performed. *Error bars* indicate S.E. *D,* Western blots showing the levels of endogenous TPX2, GFP-TPX2 WT, and GFP-TPX2 T72A in HeLa cells co-transfected with GFP-vector, GFP-TPX2 WT, or GFP-TPX2 T72A together with TPX2 siRNA targeting the 3′ UTR of TPX2 mRNA. *E*, bar graphs showing the number of cells with different mono-, bi-, or multipolar mitotic spindles in each group. Cells with mitotic spindles were fixed and stained with Cy3-conjugated tubulin for MT visualization. Knockdown of TPX2 in GFP-transfected cells results in a significant 5.4% increase in multipolar spindles *versus* control cells without TPX2 depletion. GFP-TPX2 T72A expression produces an even greater 9.8 and 7.5% increase in the percentage of cells with multipolar spindles when compared with GFP/TPX2 siRNA and GFP-TPX2 WT/TPX siRNA, respectively. $n = 3$, ANOVA test was used the compare the four groups ($p < 0.01$). The Neuman-Keuls test was used to compare the following groups: control (with control siRNA) (2.43 $\pm$ 0.41) *versus* GFP (7.94 $\pm$ 1.5), $p < 0.05$; GFP (7.94 $\pm$ 1.5) *versus* TPX2 WT (10.13 $\pm$ 1.2), NS; WT (10.13 $\pm$ 1.2) *versus* T72A (17.67 $\pm$ 3.2), $p < 0.05$; GFP (7.94 $\pm$ 1.5) *versus* T72A (17.67 $\pm$ 3.2), $p < 0.05$; group (mean $\pm$ S.E.); *, $p < 0.05$; *NS*, not significant. $n =$ at least 500 cells for each set of experiments; 3 independent experiments were performed. *Error bars* indicate S.E.

down endogenous TPX2 without altering the expression of GFP-TPX2 or GFP-TPX2 T72A (see "Experimental Procedures" and Refs. 33 and 36) for detailed information on TPX2 siRNA). For this particular experiment, we expressed GFP-TPX2 and GFP-TPX2 T72A at levels comparable with levels of endogenous TPX2 (Fig. 6*D*). Note that the total amount of ectopic and endogenous TPX2 in these samples was similar to levels of endogenous TPX2 in unmanipulated cells. We also ensured that the levels of GFP-TPX2 WT and T72A mutant expression were similar so that differences in the results would not be attributed to variations in protein expression. In agreement with previous work (6), we found that partial knockdown of TPX2 caused cells to have more multipolar spindles (Fig. 6*E*). Importantly, consistent with the first set of experiments with endogenous TPX2 (Fig. 6*C*), transfection of GFP-TPX2 T72A in the partial absence of endogenous TPX2 further increased the frequency of cells with multipolar spindles when compared with GFP-TPX2 (Fig. 6*E*) (0.25 *versus* 0.30 for the ratio of cells

with multipolar spindles/cells with bipolar spindle in experiments with no TPX2 knockdown (Fig. 6*C*) *versus* experiments with partial TPX2 knockdown (Fig. 6*E*)). Of note, in our experimental settings, GFP-TPX2 expression was not able to rescue the multipolar spindles phenotype caused by TPX2 depletion due to differences in time-dependent expression of the siRNA and cDNA constructs. In summary, abolition of Thr$^{72}$ phosphorylation caused a significant increase in the percentage of HeLa cells with multipolar spindle poles. Thus, Thr$^{72}$ phosphorylation is important for formation of a bipolar spindle.

*Phosphorylation of TPX2 at Thr$^{72}$ Regulates the Activity of Aurora A and Affects Spindle Length, a Reflective Measure of Eg5 Activity*—Tight regulation of Aurora A and Eg5 activities by TPX2 is essential for normal bipolar spindle formation (reviewed in Ref. 10). Specifically, the Aurora A binding domain on TPX2 (amino acids 1–43) allows it to interact with the kinase, resulting in kinase activation. Activated Aurora A is key for MT nucleation and organization during spindle morphogenesis. Inactive or overactivated Aurora A induces spindle abnormalities including a multipolar spindles phenotype (11, 12). In parallel, reduced motor activity of Eg5 by TPX2 is critical for MT cross-linking, sliding along MTs, and generation of outward forces for spindle pole separation at mitotic entry. Indeed, inhibition of the TPX2/Eg5 association mediated through the C-terminal of TPX2 (amino acids 711–747) causes alterations in mitotic spindle polarity, extra MT foci, and enhanced MT nucleation around chromosomes (14, 15), whereas inhibition of Eg5 with monastrol reduces the number of cells with multipolar spindles (45).

Based on the multipolar spindles phenotype of T72A-expressing cells and the facts that the same phenotype is recapitulated in cells with reduced or enhanced Aurora A activity (11, 12), or with disrupted Eg5/TPX2 interaction (*i.e.* cells with enhanced Eg5 activity) (14, 15), but attenuated in cells with Eg5 inhibited by monastrol (45), we sought to determine the activity of Aurora A and Eg5 in TPX2 T72A-expressing cells. Activation of Aurora A was determined by levels of phosphothreonine 288 (Thr(P)$^{288}$, *i.e.* activated) Aurora A using immunofluorescence and confocal microscopy, whereas Eg5 activity was monitored indirectly with MTs spindle length. Longer spindle MTs would be reflective of enhanced motor activity of Eg5 (14, 15). Using these parameters, we found that GFP-TPX2 T72A significantly enhances the levels of Thr(P)$^{288}$ Aurora A when compared with WT at the spindle poles (Fig. 7*A*). Furthermore, expression of the mutant also augments MTs spindle length, suggestive of altered Eg5 activity (Fig. 7*B*), without affecting the amount of total $\alpha$-tubulin detected on the spindle (Fig. 7*C*). Taken together, these results suggest that inability to phosphorylate TPX2 at Thr$^{72}$ results in overactivation of Aurora A and Eg5 during spindle assembly.

## DISCUSSION

In the present study, we found that TPX2 is phosphorylated by Cdk1 and Cdk2 at Thr$^{72}$ *in vitro* and *in vivo* (Figs. 1 and 4). Using homemade Abs specific for Thr(P)$^{72}$ and mass spectrometry (Figs. 1 and 2), we further discovered that Thr$^{72}$ phosphorylation peaks at M phase (Fig. 3), a stage of the cell cycle where the expression of TPX2 is the highest and Cdk1 is active. Abolishment of Thr$^{72}$ phosphorylation with the use of the T72A mutant significantly increases the proportion of cells with multipolar spindles, particularly in the absence of endogenous TPX2 (Fig. 6), and this phenotype is associated with a mislocalization of T72A (Fig. 5). Expression of TPX2 T72A also up-regulates the kinase activity of Aurora A and enhances spindle length, a correlative measure of Eg5 motor activity (Fig. 7). Deregulation of either activity has been shown to disturb formation of bipolar spindle. Thus, phosphorylation of TPX2 at Thr$^{72}$ occurs in mitotic cells, regulates TPX2 localization, and likely impacts spindle assembly via Aurora A and Eg5.

In the current literature, only three phosphorylation sites on *Xenopus* TPX2 have been functionally characterized. Echkerdt *et al.* (47) identified serine 204 in *Xenopus* TPX2 as a Plx1 (*Xenopus* Polo-like kinase 1) target. Plx1 kinase activity is required for mitotic progression in *Xenopus*. When TPX2 is phosphorylated at Ser$^{204}$ by Plx1, TPX2 activates Aurora A. Sequence comparison shows that this site is not conserved between species and no research has been done to identify equivalent phosphorylation sites in other species, including human. The two other sites that have been characterized in *Xenopus* TPX2 are tyrosine 8 and tyrosine 10 (48). These sites are conserved between *Xenopus* and human TPX2 and are in the domain that closely binds to Aurora A (49) and activates the kinase. Mutations of both Tyr$^{8}$ and Tyr$^{10}$ to alanine prevent binding of TPX2 to Aurora A, abolish Aurora A activation, and also prevent TPX2 phosphorylation by Aurora A (48). Thus, our study constitutes the first *in vivo* functional characterization of a TPX2 phosphorylation site in human cells with implication for cancers (see below).

*How Does Phosphorylation of TPX2 at Thr$^{72}$ Regulate Spindle Formation?*—The balance between structural support by TPX2 and motor force by Eg5, as well as a proper activation of Aurora A are essential for normal bipolar spindle formation. We found that the inability to phosphorylate TPX2 at Thr$^{72}$ enhances MT spindle length, a measure of the activity of Eg5. In a mutually non-exclusive scenario, we also discovered that TPX2 T72A induces hyperactivation of Aurora A. During spindle assembly, activation of Aurora A by TPX2 depends on RanGTP that mediates the release of TPX2 from the inhibitory Importin complex in the vicinity of mitotic chromosomes (reviewed in Ref. 10). As the RanGTP concentration decreases at increasing distance to mitotic chromatin, the highest concentration of Importin-free TPX2 (translated into highest Aurora A activity) is found near the chromosomes (10). The results obtained with our homemade antibodies showing that Thr(P)$^{72}$ TPX2 localizes at the cell periphery (Fig. 5, *A* and *C*), and the finding that T72A accumulates aberrantly on the mitotic spindle (Fig. 5*D*) where Aurora A activity is up-regulated (Fig. 7*A*) are all consistent with the current model of TPX2-mediated spindle assembly (10). Furthermore, because TPX2 controls the stability of Aurora A (46), an accumulation of TPX2 T72A on the spindle may prolong the stability and activation of Aurora at this location (Fig. 7*A*). Thus, deregulation of Aurora A and Eg5 activity are likely to contribute to multipolar spindles phenotype and spindle anomalies observed in GFP-TPX2 T72A-expressing cells.

That the localization of proteins involved in spindle assembly and function is tightly regulated by phosphorylation (as is

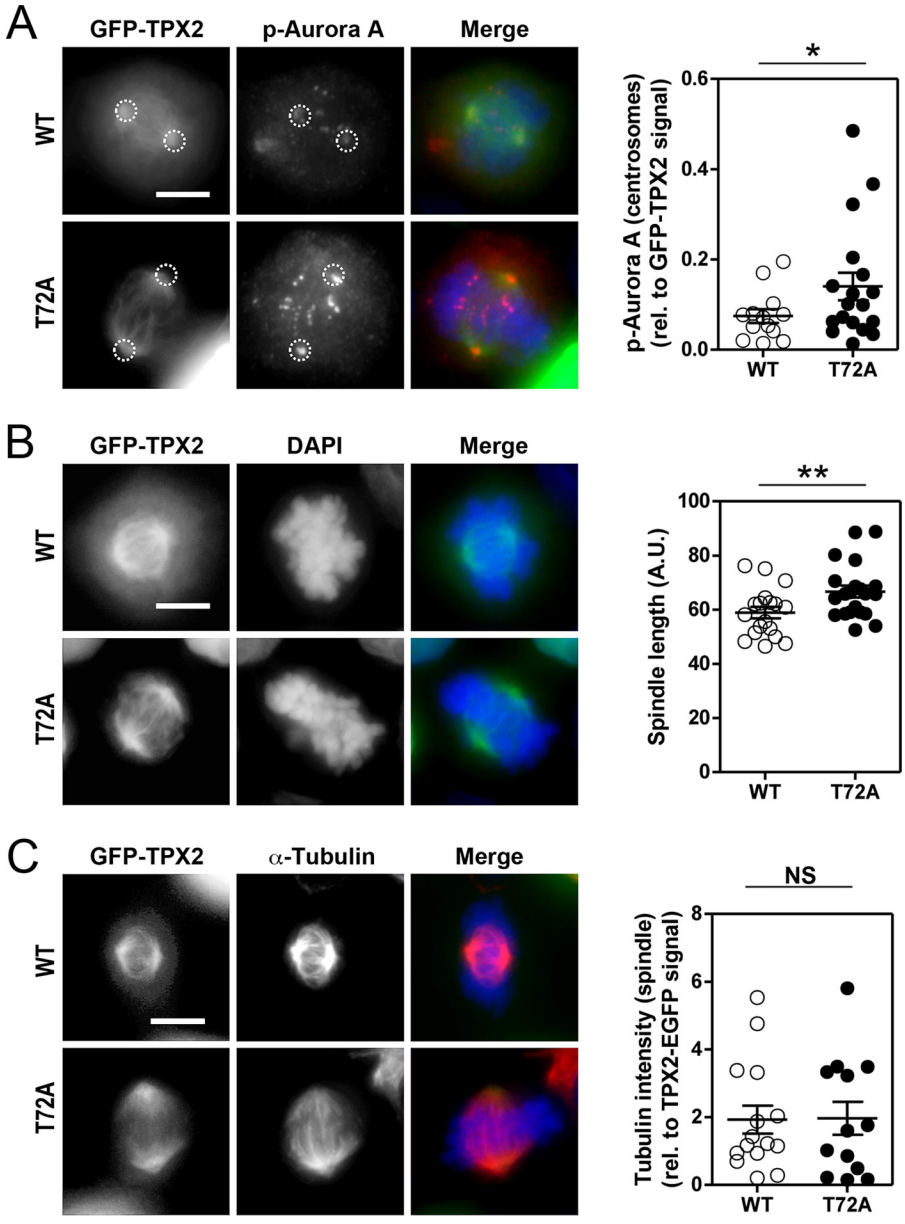


FIGURE 7. **Overactivation of Aurora A and increased spindle length, a measure of Eg5 activity, in TPX2 T72A-expressing cells.** *A–C* show 293 mitotic cells (prometaphase/metaphase) previously transfected with GFP-TPX2 WT (WT) or GFP-TPX2 T72A (T72A) expression vectors. *A*, representative photographs of WT- and T72A-transfected cells stained for Thr(P)$^{288}$, a phosphoresidue indicative of the activity of Aurora kinase A. *Dotted circles* identify the poles. Scatter plots show the P-Aurora signal at centrosomes relative to total GFP signal. GFP-TPX2 T72A induces higher Aurora A activity than GFP-TPX2 WT (GFP-TPX2 WT (0.07 $\pm$ 0.01, $n = 13$) *versus* GFP-TPX2 T72A (0.14 $\pm$ 0.03, $n = 18$); *, $p < 0.05$ by *t* test). *B*, representative photographs of the spindle length detected in mitotic 293 cells transfected with GFP-TPX2 WT or T72A. Scatter plots show the spindle length in both groups. T72A-expressing cells display longer spindles than WT-expressing cells (GFP-TPX2 WT (58.95 $\pm$ 2.12, $n = 18$) *versus* GFP-TPX2 T72A (66.67 $\pm$ 2.20, $n = 21$); **, $p < 0.01$ by *t* test). *C*, representative images of the $\alpha$-tubulin signal detected in GFP-TPX2 WT and T72A-trasnfected 293 cells. No significant difference was detected between these two groups (GFP-TPX2 WT (1.93 $\pm$ 0.41, $n = 15$) *versus* GFP-TPX2 T72A (1.97 $\pm$ 0.49, $n = 13$); *NS*, non significant by *t* test). In all the panels: the group is the mean $\pm$ S.E.. *Scale bar*, 10 $\mu$m.

shown in this study for TPX2) is not unprecedented. For instance, during interphase nucleolin is a major protein localized in the nucleoli. During mitosis, it relocalizes at the chromosome periphery (50) but once phosphorylated by CDC2, it associates with the spindle poles from prometaphase to anaphase (50–52). Nucleolin-depleted cells showed a prolonged cell cycle with misaligned chromosomes and defects in spindle organization. The staining pattern of endogenous Thr(P)$^{72}$ TPX2 is reminiscent of the pattern displayed by mitotic unphosphorylated nucleolin. These results suggest that Thr(P)$^{72}$ TPX2 may regulate spindle assembly in concert with nucleolin. How this potential regulation is linked to the Eg5-dependent and/or RanGTP/Aurora-dependent modulation of spindle assembly remains to be determined. Future studies are required to refine the mechanism(s) by which Thr$^{72}$ phosphorylation ensures bipolar spindle formation.

*Overexpression and Phosphorylation of TPX2 in Cancers*—TPX2 has been proposed as a biomarker and effector for cancer progression based on its elevated levels in numerous malignancies (lung, pancreas, ovary, bone, carcinomas, breast, cervix,

etc.) (see Table 2 of Ref. 10 for a summary of the recent large body of evidence pointing to increased expression of TPX2 in cancer cells and tissues). In addition to these "cancer-type specific" analyses, TPX2 is overexpressed in 53 of 193 (27%) microarray assays that compared gene expression profiles of various cancers with their normal tissue counterpart (13). The involvement of TPX2 in cancers has been mostly associated with deregulation of its spindle assembly actions. Indeed, among 10,000 genes overexpressed in cancers, enhanced expression of TPX2 was found to correlate best with the magnitude of chromosomal instability (53), a consequence of altered spindle function and important feature of cancers (54–56). Thus, overexpression of TPX2 in numerous malignancies, combined with its crucial function as a regulator of spindle formation and mitosis, implicate TPX2 as potential driving and/or modulatory force for carcinogenesis. Interestingly, TPX2 regulates the oncogenic Aurora A kinase. Like *tpx2*, *aurora A* maps to chromosome 20q and the two genes seem to be co-overexpressed in colorectal cancers (13, 57, 58). In light of TPX2 being an activator of Aurora A, the two proteins, if co-overexpressed, may form an oncogenic unit that is more pathogenic, and perhaps more malignant, than increased levels of either TPX2 or Aurora A alone (13). In the same perspective, overactivation of Aurora A by aberrant phosphorylation of TPX2 at Thr$^{72}$, as proposed in our work (Fig. 7), may contribute to unravel the cancers-associated roles of TPX2. In addition to HeLa cells (this study), the CST curation database of PhosphoSite obtained by mass spectrometry reveals that TPX2 is also phosphorylated at Thr$^{72}$ in human gastric and lung cancer cell lines. Furthermore, a somatic mutation compiled on COSMIC (Catalogue of Somatic Mutation in Cancer) at base pair 214 (A → G) changing amino acid Thr$^{72}$ into an alanine (T72A mutation) is found in a human endometrium carcinoma. Additional phosphorylation-dead mutations at Thr$^{72}$ are likely to be discovered in the future. Thus, the use of TPX2 T72A mutant in our experiments appears to be highly relevant for the study of TPX2 under physiological and cancer conditions.

Discovered more than 17 years ago, TPX2 has emerged as an essential factor for spindle assembly and mitosis in human cells. As altered spindle assembly underlies chromosomal instability and TPX2 misregulation has been associated with numerous cancers, our study uncovers novel aspects of the spindle biology of TPX2, thereby refining its role as a marker and therapeutic target in cancers. Recently, we discovered the first nuclear roles for TPX2 in the amplification of phosphorylated histone variant H2AX (γ-H2AX), and chromatin remodeling (33, 36). γ-H2AX is a key molecule that mounts the DNA damage response so essential for cells to repair their damaged DNA, survive, or self-eliminate to prevent genomic instability. Inability to mount and control a proper DNA damage response, as observed in cells with deregulated TPX2 (33, 36), contributes to genomic instability and may result in several types of cancers. Therefore, TPX2 deregulation may not only participate into chromosome instability but also in other forms of genomic instability in cancer cells (59). Our discovery of TPX2 regulation by phosphorylation at Thr$^{72}$ opens a new perspective to study both interphase and mitotic functions of TPX2 with implications for cancer research. Future experiments looking at other phosphorylation sites will shed new light onto the physiological and pathological roles of TPX2 in cancers.

## REFERENCES


1. Wittmann, T., Boleti, H., Antony, C., Karsenti, E., and Vernos, I. (1998) Localization of the kinesin-like protein Xklp2 to spindle poles requires a leucine zipper, a microtubule-associated protein, and dynein. *J. Cell Biol.* **143,** 673–685
2. Heidebrecht, H. J., Buck, F., Steinmann, J., Sprenger, R., Wacker, H. H., and Parwaresch, R. (1997) p100: a novel proliferation-associated nuclear protein specifically restricted to cell cycle phases S, $G_2$, and M. *Blood* **90,** 226–233
3. Schatz, C. A., Santarella, R., Hoenger, A., Karsenti, E., Mattaj, I. W., Gruss, O. J., and Carazo-Salas, R. E. (2003) Importin α-regulated nucleation of microtubules by TPX2. *EMBO J.* **22,** 2060–2070
4. Brunet, S., Sardon, T., Zimmerman, T., Wittmann, T., Pepperkok, R., Karsenti, E., and Vernos, I. (2004) Characterization of the TPX2 domains involved in microtubule nucleation and spindle assembly in *Xenopus* egg extracts. *Mol. Biol. Cell* **15,** 5318–5328
5. Gruss, O. J., Wittmann, M., Yokoyama, H., Pepperkok, R., Kufer, T., Silljé, H., Karsenti, E., Mattaj, I. W., and Vernos, I. (2002) Chromosome-induced microtubule assembly mediated by TPX2 is required for spindle formation in HeLa cells. *Nat. Cell Biol.* **4,** 871–879
6. Garrett, S., Auer, K., Compton, D. A., and Kapoor, T. M. (2002) hTPX2 is required for normal spindle morphology and centrosome integrity during vertebrate cell division. *Curr. Biol.* **12,** 2055–2059
7. Aguirre-Portolés, C., Bird, A. W., Hyman, A., Cañamero, M., Pérez de Castro, I., and Malumbres, M. (2012) Tpx2 controls spindle integrity, genome stability, and tumor development. *Cancer Res.* **72,** 1518–1528
8. Stewart, S., and Fang, G. (2005) Anaphase-promoting complex/cyclosome controls the stability of TPX2 during mitotic exit. *Mol. Cell Biol.* **25,** 10516–10527
9. Petry, S., Groen, A. C., Ishihara, K., Mitchison, T. J., and Vale, R. D. (2013) Branching microtubule nucleation in *Xenopus* egg extracts mediated by augmin and TPX2. *Cell* **152,** 768–777
10. Neumayer, G., Belzil, C., Gruss, O. J., and Nguyen, M. D. (2014) TPX2: of spindle assembly, DNA damage response, and cancer. *Cell Mol. Life Sci.* **71,** 3027–3047
11. Asteriti, I. A., Giubettini, M., Lavia, P., and Guarguaglini, G. (2011) Aurora-A inactivation causes mitotic spindle pole fragmentation by unbalancing microtubule-generated forces. *Mol. Cancer* **10,** 131
12. Anand, S., Penrhyn-Lowe, S., and Venkitaraman, A. R. (2003) AURORA-A amplification overrides the mitotic spindle assembly checkpoint, inducing resistance to Taxol. *Cancer Cell* **3,** 51–62
13. Asteriti, I. A., Rensen, W. M., Lindon, C., Lavia, P., and Guarguaglini, G. (2010) The Aurora-A/TPX2 complex: a novel oncogenic holoenzyme? *Biochim. Biophys. Acta* **1806,** 230–239
14. Ma, N., Titus, J., Gable, A., Ross, J. L., and Wadsworth, P. (2011) TPX2 regulates the localization and activity of Eg5 in the mammalian mitotic spindle. *J. Cell Biol.* **195,** 87–98
15. Eckerdt, F., Eyers, P. A., Lewellyn, A. L., Prigent, C., and Maller, J. L. (2008) Spindle pole regulation by a discrete Eg5-interacting domain in TPX2. *Curr. Biol.* **18,** 519–525
16. Perkins, D. N., Pappin, D. J., Creasy, D. M., and Cottrell, J. S. (1999) Probability-based protein identification by searching sequence databases using mass spectrometry data. *Electrophoresis* **20,** 3551–3567
17. Hornbeck, P. V., Kornhauser, J. M., Tkachev, S., Zhang, B., Skrzypek, E., Murray, B., Latham, V., and Sullivan, M. (2012) PhosphoSitePlus: a comprehensive resource for investigating the structure and function of experimentally determined post-translational modifications in man and mouse. *Nucleic Acids Res.* **40,** D261-D270
18. Wittmann, T., Wilm, M., Karsenti, E., and Vernos, I. (2000) TPX2, A novel *Xenopus* MAP involved in spindle pole organization. *J. Cell Biol.* **149,** 1405–1418
19. Franz-Wachtel, M., Eisler, S. A., Krug, K., Wahl, S., Carpy, A., Nordheim, A., Pfizenmaier, K., Hausser, A., and Macek, B. (2012) Global detection of protein kinase D-dependent phosphorylation events in nocodazole-

treated human cells. *Mol. Cell Proteomics* **11,** 160–170
20. Grosstessner-Hain, K., Hegemann, B., Novatchkova, M., Rameseder, J., Joughin, B. A., Hudecz, O., Roitinger, E., Pichler, P., Kraut, N., Yaffe, M. B., Peters, J. M., and Mechtler, K. (2011) Quantitative phospho-proteomics to investigate the polo-like kinase 1-dependent phospho-proteome. *Mol. Cell Proteomics* **10,** 10.1074/mcp.M111.008540
21. Kettenbach, A. N., Schweppe, D. K., Faherty, B. K., Pechenick, D., Pletnev, A. A., and Gerber, S. A. (2011) Quantitative phosphoproteomics identifies substrates and functional modules of Aurora and Polo-like kinase activities in mitotic cells. *Sci. Signal.* **4,** rs5
22. Olsen, J. V., Vermeulen, M., Santamaria, A., Kumar, C., Miller, M. L., Jensen, L. J., Gnad, F., Cox, J., Jensen, T. S., Nigg, E. A., Brunak, S., and Mann, M. (2010) Quantitative phosphoproteomics reveals widespread full phosphorylation site occupancy during mitosis. *Sci. Signal.* **3,** ra3
23. Malik, R., Lenobel, R., Santamaria, A., Ries, A., Nigg, E. A., and Körner, R. (2009) Quantitative analysis of the human spindle phosphoproteome at distinct mitotic stages. *J. Proteome Res.* **8,** 4553–4563
24. Chi, Y., Welcker, M., Hizli, A. A., Posakony, J. J., Aebersold, R., and Clurman, B. E. (2008) Identification of CDK2 substrates in human cell lysates. *Genome Biol.* **9,** R149
25. Nousiainen, M., Silljé, H. H., Sauer, G., Nigg, E. A., and Körner, R. (2006) Phosphoproteome analysis of the human mitotic spindle. *Proc. Natl. Acad. Sci. U.S.A.* **103,** 5391–5396
26. Dephoure, N., Zhou, C., Villén, J., Beausoleil, S. A., Bakalarski, C. E., Elledge, S. J., and Gygi, S. P. (2008) A quantitative atlas of mitotic phosphorylation. *Proc. Natl. Acad. Sci. U.S.A.* **105,** 10762–10767
27. Chen, R. Q., Yang, Q. K., Lu, B. W., Yi, W., Cantin, G., Chen, Y. L., Fearns, C., Yates, J. R., 3rd, and Lee, J. D. (2009) CDC25B mediates rapamycin-induced oncogenic responses in cancer cells. *Cancer Res.* **69,** 2663–2668
28. Mayya, V., Lundgren, D. H., Hwang, S. I., Rezaul, K., Wu, L., Eng, J. K., Rodionov, V., and Han, D. K. (2009) Quantitative phosphoproteomic analysis of T cell receptor signaling reveals system-wide modulation of protein-protein interactions. *Sci. Signal.* **2,** ra46
29. Weber, C., Schreiber, T. B., and Daub, H. (2012) Dual phosphoproteomics and chemical proteomics analysis of erlotinib and gefitinib interference in acute myeloid leukemia cells. *J. Proteomics* **75,** 1343–1356
30. Shiromizu, T., Adachi, J., Watanabe, S., Murakami, T., Kuga, T., Muraoka, S., and Tomonaga, T. (2013) Identification of missing proteins in the neXtProt database and unregistered phosphopeptides in the PhosphoSitePlus database as part of the Chromosome-Centric Human Proteome Project. *J. Proteome Res.* **12,** 2414–2421
31. Zhou, H., Di Palma, S., Preisinger, C., Peng, M., Polat, A. N., Heck, A. J., and Mohammed, S. (2013) Toward a comprehensive characterization of a human cancer cell phosphoproteome. *J. Proteome Res.* **12,** 260–271
32. Daub, H., Olsen, J. V., Bairlein, M., Gnad, F., Oppermann, F. S., Körner, R., Greff, Z., Kéri, G., Stemmann, O., and Mann, M. (2008) Kinase-selective enrichment enables quantitative phosphoproteomics of the kinome across the cell cycle. *Mol. Cell* **31,** 438–448
33. Neumayer, G., Helfricht, A., Shim, S. Y., Le, H. T., Lundin, C., Belzil, C., Chansard, M., Yu, Y., Lees-Miller, S. P., Gruss, O. J., van Attikum, H., Helleday, T., and Nguyen, M. D. (2012) Targeting protein for xenopus kinesin-like protein 2 (TPX2) regulates γ-histone 2AX (γ-H2AX) levels upon ionizing radiation. *J. Biol. Chem.* **287,** 42206–42222
34. Nguyen, M. D., Larivière, R. C., and Julien, J. P. (2001) Deregulation of Cdk5 in a mouse model of ALS: toxicity alleviated by perikaryal neurofilament inclusions. *Neuron* **30,** 135–147
35. Kufer, T. A., Silljé, H. H., Körner, R., Gruss, O. J., Meraldi, P., and Nigg, E. A. (2002) Human TPX2 is required for targeting Aurora-A kinase to the spindle. *J. Cell Biol.* **158,** 617–623
36. Neumayer, G., and Nguyen, M. D. (2014) TPX2 impacts acetylation of histone H4 at lysine 16: implications for DNA damage response. *Plos One* **9,** e110994
37. Trieselmann, N., Armstrong, S., Rauw, J., and Wilde, A. (2003) Ran modulates spindle assembly by regulating a subset of TPX2 and Kid activities including Aurora A activation. *J. Cell Sci.* **116,** 4791–4798
38. Havlícek, L., Hanus, J., Veselý, J., Leclerc, S., Meijer, L., Shaw, G., and Strnad, M. (1997) Cytokinin-derived cyclin-dependent kinase inhibitors: synthesis and cdc2 inhibitory activity of olomoucine and related compounds. *J. Med. Chem.* **40,** 408–412
39. De Azevedo, W. F., Leclerc, S., Meijer, L., Havlicek, L., Strnad, M., and Kim, S. H. (1997) Inhibition of cyclin-dependent kinases by purine analogues: crystal structure of human cdk2 complexed with roscovitine. *Eur. J. Biochem.* **243,** 518–526
40. Meijer, L., Borgne, A., Mulner, O., Chong, J. P., Blow, J. J., Inagaki, N., Inagaki, M., Delcros, J. G., and Moulinoux, J. P. (1997) Biochemical and cellular effects of roscovitine, a potent and selective inhibitor of the cyclin-dependent kinases cdc2, cdk2 and cdk5. *Eur. J. Biochem.* **243,** 527–536
41. Tsai, L. H., Delalle, I., Caviness, V. S., Jr., Chae, T., and Harlow, E. (1994) P35 is a neural-specific regulatory subunit of cyclin-dependent kinase-5. *Nature* **371,** 419–423
42. Zheng, M., Leung, C. L., and Liem, R. K. (1998) Region-specific expression of cyclin-dependent kinase 5 (cdk5) and its activators, p35 and p39, in the developing and adult rat central nervous system. *J. Neurobiol.* **35,** 141–159
43. Sharma, P., Sharma, M., Amin, N. D., Albers, R. W., and Pant, H. C. (1999) Regulation of cyclin-dependent kinase 5 catalytic activity by phosphorylation. *Proc. Natl. Acad. Sci. U.S.A.* **96,** 11156–11160
44. Skoufias, D. A., Indorato, R. L., Lacroix, F., Panopoulos, A., and Margolis, R. L. (2007) Mitosis persists in the absence of Cdk1 activity when proteolysis or protein phosphatase activity is suppressed. *J. Cell Biol.* **179,** 671–685
45. Kapoor, T. M., Mayer, T. U., Coughlin, M. L., and Mitchison, T. J. (2000) Probing spindle assembly mechanisms with monastrol, a small molecule inhibitor of the mitotic kinesin, Eg5. *J. Cell Biol.* **150,** 975–988
46. Giubettini, M., Asteriti, I. A., Scrofani, J., De Luca, M., Lindon, C., Lavia, P., and Guarguaglini, G. (2011) Control of Aurora-A stability through interaction with TPX2. *J. Cell Sci.* **124,** 113–122
47. Eckerdt, F., Pascreau, G., Phistry, M., Lewellyn, A. L., DePaoli-Roach, A. A., and Maller, J. L. (2009) Phosphorylation of TPX2 by Plx1 enhances activation of Aurora A. *Cell Cycle* **8,** 2413–2419
48. Eyers, P. A., and Maller, J. L. (2004) Regulation of Xenopus Aurora A activation by TPX2. *J. Biol. Chem.* **279,** 9008–9015
49. Bayliss, R., Sardon, T., Vernos, I., and Conti, E. (2003) Structural basis of Aurora-A activation by TPX2 at the mitotic spindle. *Mol. Cell* **12,** 851–862
50. Ma, N., Matsunaga, S., Takata, H., Ono-Maniwa, R., Uchiyama, S., and Fukui, K. (2007) Nucleolin functions in nucleolus formation and chromosome congression. *J. Cell Sci.* **120,** 2091–2105
51. Peter, M., Nakagawa, J., Dorée, M., Labbé, J. C., and Nigg, E. A. (1990) Identification of major nucleolar proteins as candidate mitotic substrates of cdc2 kinase. *Cell* **60,** 791–801
52. Belenguer, P., Caizergues-Ferrer, M., Labbé, J. C., Dorée, M., and Amalric, F. (1990) Mitosis-specific phosphorylation of nucleolin by p34cdc2 protein kinase. *Mol. Cell. Biol.* **10,** 3607–3618
53. Carter, S. L., Eklund, A. C., Kohane, I. S., Harris, L. N., and Szallasi, Z. (2006) A signature of chromosomal instability inferred from gene expression profiles predicts clinical outcome in multiple human cancers. *Nat. Genet.* **38,** 1043–1048
54. Thompson, S. L., Bakhoum, S. F., and Compton, D. A. (2010) Mechanisms of chromosomal instability. *Curr. Biol.* **20,** R285–R295
55. Hanahan, D., and Weinberg, R. A. (2000) The hallmarks of cancer. *Cell* **100,** 57–70
56. Hanahan, D., and Weinberg, R. A. (2011) Hallmarks of cancer: the next generation. *Cell* **144,** 646–674
57. Bischoff, J. R., Anderson, L., Zhu, Y., Mossie, K., Ng, L., Souza, B., Schryver, B., Flanagan, P., Clairvoyant, F., Ginther, C., Chan, C. S., Novotny, M., Slamon, D. J., and Plowman, G. D. (1998) A homologue of *Drosophila* aurora kinase is oncogenic and amplified in human colorectal cancers. *EMBO J.* **17,** 3052–3065
58. Sillars-Hardebol, A. H., Carvalho, B., Tijssen, M., Beliën, J. A., de Wit, M., Delis-van Diemen, P. M., Pontén, F., van de Wiel, M. A., Fijneman, R. J., and Meijer, G. A. (2012) TPX2 and AURKA promote 20q amplicon-driven colorectal adenoma to carcinoma progression. *Gut.* **61,** 1568–1575
59. Pérez de Castro, I., and Malumbres, M. (2012) Mitotic stress and chromosomal instability in cancer: the case for TPX2. *Genes Cancer* **3,** 721–730